

# FINAL PROJECT REPORT #00042134-02-2A-2

GRANT: DTRT13-G-UTC45  
Project Period: 5/15/2017 – 6/30/18

## Passive Wireless Sensors for Monitoring Behavior of Recycled Aggregate Concrete

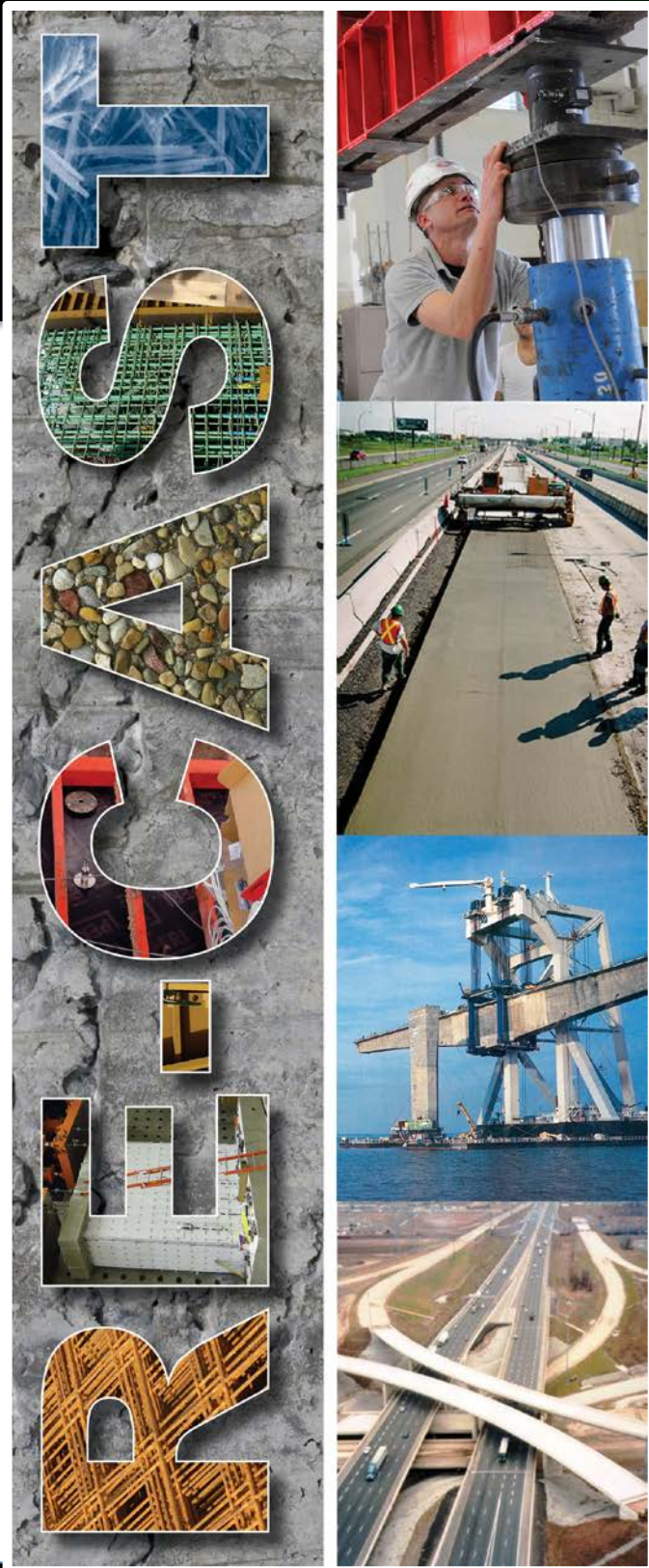
Participating Consortium Member:  
University of Illinois Urbana-Champaign

Author:

**David Lange, Ph.D.**

*Professor*

*Dept. of Civil, Environ. Engineering  
University of Illinois Urbana-Champaign*



**RE-CAST:**  
REsearch on Concrete Applications for  
Sustainable Transportation  
Tier 1 University Transportation Center



## ***DISCLAIMER***

The contents of this report reflect the views of the authors, who are responsible for the facts and the accuracy of the information presented herein. This document is disseminated under the sponsorship of the U.S. Department of Transportation's University Transportation Centers Program, in the interest of information exchange. The U.S. Government assumes no liability for the contents or use thereof.

**TECHNICAL REPORT DOCUMENTATION PAGE**

<b>1. Report No.</b> RECAST UTC # 00042134-02-2A-2	<b>2. Government Accession No.</b>	<b>3. Recipient's Catalog No.</b>
<b>4. Title and Subtitle</b> Passive Wireless Sensors for Monitoring Behavior of Recycled Aggregate Concrete	<b>5. Report Date</b> August 2018	
	<b>6. Performing Organization Code:</b>	
<b>7. Author(s)</b> D. Lange	<b>8. Performing Organization Report No.</b> Project # 00042134-02-2A-2	
<b>9. Performing Organization Name and Address</b> RE-CAST – UIUC 2129b Newmark Civil Engineering Bldg, 205 N. Mathews Urbana Illinois 61801	<b>10. Work Unit No.</b>	
	<b>11. Contract or Grant No.</b> USDOT: DTRT13-G-UTC45	
<b>12. Sponsoring Agency Name and Address</b> Office of the Assistant Secretary for Research and Technology U.S. Department of Transportation 1200 New Jersey Avenue, SE Washington, DC 20590	<b>13. Type of Report and Period Covered:</b> Final Report Period: 5/15/2017 – 6/30/18	
	<b>14. Sponsoring Agency Code:</b>	
<b>15. Supplementary Notes</b> The investigation was conducted in cooperation with the U. S. Department of Transportation. A supplementary report will be added to this project in December 2018.		
<b>16. Abstract</b> This project studied the feasibility of applying new RFID technology – particularly passive tag technology – to infrastructure projects that incorporate recycled concrete aggregates. Our goals were to advance the technology for passive RFID wireless system for embedment in concrete to monitor the behavior of the material under loading, and other structural health monitoring scenarios. RFID tabs with temperature and strain measurement were studied, and the performance constraints that affect data logging were assessed. When RFID tags are embedded into concrete, the attenuation of the electromagnetic wave through concrete is correlated with the embedment depth, moisture content, concrete density, and aggregate mineralogy. The study considered these and other variables that affect passive RFID systems and suggest an approximate equation to estimate the attenuation. The project assessed the accuracy and data logging rates to validate the strain readings from passive RFID systems with other independent instruments. The early age monitoring of recycled aggregate concrete will be conducted with the RFID system. This project is a precursor to a field test at O’Hare Int’l Airport to demonstrate the survivability of RFID systems for real-world operation in aggressive weather conditions.		
<b>17. Key Words</b> RFID technology, passive tag technology, recycled concrete aggregates	<b>18. Distribution Statement</b> No restrictions. This document is available to the public.	
<b>19. Security Classification (of this report)</b> Unclassified	<b>20. Security Classification (of this page)</b> Unclassified	<b>21. No of Pages</b> 18

## TABLE OF CONTENTS

TABLE OF CONTENTS .....	1
CHAPTER 1 – Introduction .....	2
1.1 Background.....	2
1.2 Literature review.....	3
1.3 Objectives and Goals .....	4
CHAPTER 2 – Experiments.....	5
2.1 RFID wireless sensor system design and performance evaluation.....	5
2.2 RFID strain measurement implementation of aluminum and concrete beam .....	5
2.3 Experimental verification of electromagnetic attenuation and depth dependence in concrete.....	6
CHAPTER 3 – Results and discussion.....	7
CHAPTER 3 – Findings .....	12
Reference .....	13

## CHAPTER 1 – Introduction

### 1.1 Background

The continuous and reliable operation of critical infrastructure is crucial for safety and economic prosperity, and structural health monitoring (SHM) is an attractive solution in civil engineering for continuous evaluation of infrastructures safety. SHM includes condition monitoring of structures, damage detection, structural integrity assessment, and structural failure prevention<sup>1</sup>. The utilization of sensing instrumentation within the structures is useful for monitoring long-term conditions of infrastructures<sup>2</sup>. There are some issues to be considered for SHM such as the selection of sensors, the cost, the number and location of sensors, energy supply, data collection, transmission and analysis and environmental influence<sup>1</sup>. Among them, the selection of sensors involves sensor accuracy, sensitivity, range, stability, and compensation for environmental parameters change<sup>3</sup>.

The data measured by sensors can be transmitted by coaxial wires, but the wires installation is expensive and labor intensive. For example, it has been estimated that the cost excess cost per sensing channel for SHM in tall buildings may be as much as \$5000<sup>4</sup>, and Tsing Ma bridge in Hong Kong spent more than \$8 million for 350 sensing channels<sup>5</sup>. Moreover, traditional wired sensor systems have difficulties in maintaining the wiring system in a harsh environment, and it is challenging and time-consuming to manage a large number of data if a dense array of wired sensors is deployed. In recent years, wireless sensor networks (WSNs) are becoming alternatives to traditional wired monitoring systems, attributing to the capability of assessing the physical conditions of the structural systems with low cost and instrumentation time, and autonomous data acquisition<sup>5</sup>. A wireless sensor consists of three functional modules including a computing core, a wireless communication subsystem, and a data acquisition subsystem which can convert an analog signal to digital data<sup>6</sup>.

A significant concern of embedded wireless sensors relates to sensors powering. Current wireless sensors usually utilize an external power source, for example, batteries. However, batteries typically have a shorter life than the infrastructures in which the sensors embedded, and battery replacement is difficult or impossible in some locations. The battery technology is developing stagnantly comparing with the computing performance, leading to a reduction in battery life<sup>7</sup>. Therefore, capturing electric energy is necessary from the ambient environment, and the power harvesting source includes heat, wind, flowing water, solar energy, vibration, and electromagnetic waves.

Radio Frequency Identification (RFID) technology has first been used for identification and tracking based on its unique identification and recently, it has emerged as a compelling option for many applications including construction materials handling and inventory management. The reader and tags communicate using electromagnetic waves, and data are transmitted by modulating the carrier wave. RFID tags can be either active or passive. Active tags have external power sources, usually batteries. RFID technology can also make passive sensors with no need for the battery or wired connections<sup>8</sup>. The energy consumed by the passive tags is from the electromagnetic wave sent by the reader antenna, and hence no external energy source or physical connection is required. Physical information monitoring of the structures can be achieved through processing of the signals in the reader-tag communications<sup>9</sup>. Advancements in micro-electromechanical sensors and systems (MEMS) make it possible to embed wireless sensors directly into the construction materials and monitor infrastructures continuously from manufacturing to operating<sup>10</sup>. MEMS combine mechanical and electrical components in  $\mu\text{m}$  size, and

sensors and electronics are integrated on the same device. These new-generation sensors have compact forms and low cost, and microprocessors need a relatively low power supply to achieve autonomous computing. Various sensors such as temperature sensors, moisture content sensors, and strain sensors can be integrated with the wireless devices so that the measurement of various aspects of physical conditions within infrastructures can be achieved.

RFID technology can contribute to building a low-cost and passive wireless sensor network and deploying massively distributed sensors can become practical. RFID-based sensors can be integrated into the commercial RFID systems. A strain gauge is inexpensive and easy to install for structural health monitoring, and strain variation can be used to detect potential damage to the structure. More parameters can be monitored by passive RFID-based sensors such as cracks, corrosion, moisture, and temperature.

The study aims at developing sustainable concrete materials for infrastructure applications, and RFID technology can be used to improve the performance of concrete infrastructure. Being eco-friendly and cost-saving, the recycled aggregate can be used to replace the natural aggregate, but the performance needs to be evaluated. For instance, the use of recycled concrete aggregate can raise concern about shrinkage and volume stability. RFID sensor technology can contribute to the acceptance of recycled concrete because it provides a capability to be embedded in concrete pavements and structures and can be monitored using wireless technology.

## **1.2 Literature review**

Radio frequency identification (RFID) is a wireless technology for communication. RFID can be used to identify or track specific targets, and relevant data can be read and written through electromagnetic waves. Therefore, the identification system and the particular targets do not require mechanical or optical contact. One of the early applications of RFID technology was invented in the 1970s, and it was a passive transponder with memory for a toll road. RFID techniques became widespread for commercial applications from inventory management to toll collection, supply chain tracking, and ID card access in the early 2000s.

A radio frequency identification system is comprised of hardware and software components, and the hardware component includes readers (interrogators) and tags (labels). Tags are attached to objects, and a reader transmits a signal to the tags and receives the response with information through a two-way radio. Tags have a unique serial number so that readers can identify every tag within the range. Tags could be read-only or read/write, and specific data of objects can be written into read/write tags. RFID tags have an integrated circuit to store information and modulate/demodulate the radio signal. The signal is received and transmitted by the antenna of tags.

RFID systems can be classified by the power supply mode of tags, the RFID frequency bands, and communication mechanisms. There are three kinds of tags: active, passive, and semi-active (battery-assisted passive). Active and semi-active tags have a battery on board, and passive tags have no battery. Active tags transmit signals periodically while semi-active tags will be activated in the range of RFID readers. Passive tags absorb energy from the electromagnetic field transmitted by readers and supply power for themselves. The communication mechanisms of RFID systems relate to the frequency of radio signals used by readers and tags. Two most commonly used communication ways are inductive coupling and backscatter coupling.

Researchers have explored a range of practical RFID applications in concrete. Environmental sensors for temperature and relative humidity have been developed utilizing available commercial products. An RFID transponder, i-Q32T tag from IDENTEC SOLUTIONS was used to measure the temperature of in-situ concrete<sup>11</sup>. Other humidity sensors for passive RFID systems are investigated<sup>12 13 14 15</sup>. Water content can also be monitored in real time through the passive RFID embedded sensors<sup>16</sup>. Passive RFID temperature sensors have been demonstrated<sup>17 18 19</sup>. RFID tags have been integrated with conductive surface sensors to detect cracks of concrete<sup>20</sup>. In addition, large displacements have been measured wirelessly using a printed stretchable RFID tag<sup>21</sup>. The resistance change during stretching was examined by the passive RFID system. Various RFID passive sensors have been developed to for crack monitoring due to mechanical and environmental process<sup>22 23 24 25</sup>. Displacement can also be monitored<sup>26 27</sup>. RFID tags can also be used for detecting reinforcing bar corrosion in bridge decks<sup>28</sup>. There are some commercially available RFID applications for corrosion detection<sup>29 30</sup>. Half-cell potential in the concrete could be monitored by the change of the resonant characteristics of the LC circuit in the sensor<sup>31</sup>. More corrosion RFID sensors have been explored<sup>32 33 34</sup>.

Although the great potential of passive RFID sensors has been demonstrated by these studies, there are a few tradeoffs of passive RFID tags including high required signal, measurements only in the field of the reader, small range, few numbers of multi-tag reading, and small data storage. Wireless signals may be blocked by metals and liquids due to electromagnetic interference. RFID does not work properly when the tags are surrounded by metals or liquids. Passive UHF RFID temperature sensors have been embedded in the fresh concrete to monitor hydration<sup>35</sup> and under performance tests to determine the effect of snow and ice on the surface of the tag<sup>36</sup>. Although the reasonable measurements demonstrated the reliable performance of these RFID systems in low-temperature conditions, the RFID tags may have durability issues due to mechanical disruption or electronic corrosion.

### **1.3 Objectives and Goals**

This project studied the feasibility of applying new RFID technology – particularly passive tag technology – to infrastructure projects that incorporate recycled concrete aggregates. Our goals were to advance the technology for passive RFID wireless system for embedment in concrete to monitor the behavior of the material under loading, and other structural health monitoring scenarios. RFID tabs with temperature and strain measurement were studied, and the performance constraints that affect data logging were assessed. When RFID tags are embedded into concrete, the attenuation of the electromagnetic wave through concrete is correlated with the embedment depth, moisture content, concrete density, and aggregate mineralogy. The study considered these and other variables that affect passive RFID systems and suggest an approximate equation to estimate the attenuation. The project assessed the accuracy and data logging rates to validate the strain readings from passive RFID systems with other independent instruments. The early age monitoring of recycled aggregate concrete will be conducted with the RFID system. This project is a precursor to a field test at O'Hare Int'l Airport to demonstrate the survivability of RFID systems for real-world operation in aggressive weather conditions.



## CHAPTER 2 – Experiments

### 2.1 RFID wireless sensor system design and performance evaluation

RFID equipment is provided by PHASE IV ENGINEERING INC. A custom Micro-Measurements transducer class full-bridge strain gauge has been used in the passive wireless system. These gauges are open-faced modified Karma-alloy patterns constructed on a thin, laminated, polyimide-film backing and they are encapsulated. Components of RFID system includes RFID electronics, flex cable, RFID reader, and the antenna connected to the reader. The assembly of the RFID system is also shown in Figure 2-1. Strain sensor installation is essential to the accurate measurements. Surface preparation is required before the sensor installation, and instant mix epoxy is selected as the adhesive. A strain gauge is connected to the flex cable with Kester SN 60% PB 40%, 0.31 in Rosin Core solder. Afterwards, the end of the flex cable can be connected to the connector on the RFID electronics board.

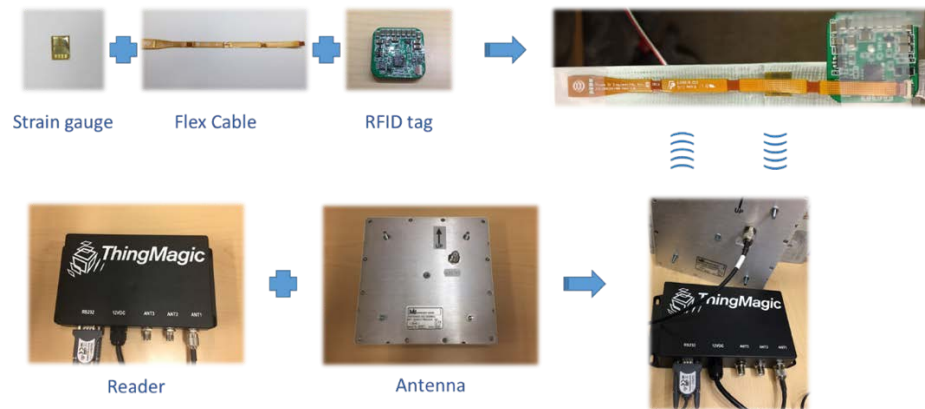


Figure 2-1. Assembly of the RFID system.

### 2.2 RFID strain measurement implementation of aluminum and concrete beam

An aluminum alloy beam ( $16.5in \times 1in \times 0.25in$ ) was rigidly clamped at its fixed end. Single point load applied by weights through the hole near the free end of the cantilever beam. An RFID strain gauge and a conventional wired strain gauge, Micro-Measurements C2A-06-250LW-120 were installed on the surface of the aluminum beam, 6.75 inches away from the point load. The wired strain gauge was plugged into a National Instruments (NI) 9235 module, and the strain data were collected by an NI compact data acquisition system (cDAQ) 9178. RFID strain gauge was attached to the surface of the concrete beam using instant mix epoxy, and a Texas Measurements type PFL-30-11-3LT concrete wired strain gauge was also installed for comparison. The wired strain gauge has a length of 30 mm, while the RFID strain gauge is much shorter with a length of 7.9 mm, shown in Figure 2-2. The concrete beam is  $12in \times 3in \times 3in$ , with  $w/cm = 0.35$ , and 20% fly ash substitutes for cement.





Figure 2-2. RFID and wired strain gauges installed on the surface of Aluminum cantilever the concrete beam.

In Figure 2-3, the packaging technology was developed so that the strain sensors can be introduced into concrete. A 6 in by 1 in by 1/8 in Plexiglas substrate was used, and notches were cut for strong adhesion. Epoxy is used to protect the strain gauge and the flex cable, and a plastic enclosure can protect the RFID sensor from moisture. A humidity sensor has also been embedded in the concrete and protected by the Gore-Tex.



Figure 2-3. Packaging concept to engage concrete in embedded applications.

### 2.3 Experimental verification of electromagnetic attenuation and depth dependence in concrete

The electromagnetic attenuation and depth dependence of tags reading were conducted with the experiment setup, shown in Figure 2-4. A piece of cardboard is covered with aluminum foil, and the RFID signal cannot be received with the cardboard in between. An opening is cut fit for concrete samples. The gaps are covered by the aluminum tape. The electromagnetic attenuation is affected by the degree of saturation of concrete, so a certain degree of saturation was obtained by a moisture conditioning scheme<sup>37</sup>. The degree of saturation was determined by the water weight increase, and the uniform humidity was achieved by one-week aluminum foil seal conditioning.

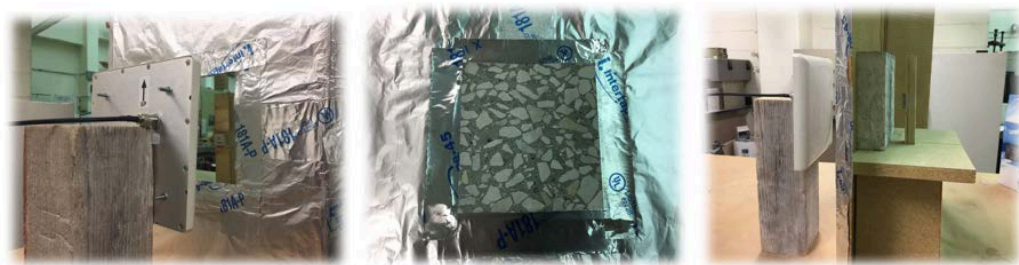


Figure 2-4. Setup to measure attenuation through samples varying in thickness, moisture, and composition.

### CHAPTER 3 – Results and discussion

RFID tags are interrogated by the RFID reader, and the data saved in the memory will be accessed. To extend the read range and improve the sensor accuracy, a circuit on the RFID board stores energy. The sensor won't transmit a sensor reading until there is enough energy stored to power the sensor circuit fully. It will cause delays in getting sensor reading – especially for the first read. 5-sec lag time is common for the first read, and 2-second read interval is the fastest. The store-up energy will vanish once the reader stops searching tags.

Received signal strength indicator (RSSI) is a measurement of the power present in a received radio signal. The magnitude of RSSI can determine if there is enough signal to get a good wireless connection. According to Friis free-space equation, the received power is inversely proportional to the square of the distance in the free space assuming that isotropic transmit antenna and a point source. As the reader moved away from the tag, the RSSI value went lower, shown in Figure 3-1, except that RSSI at 9 inches increased. Our RFID system frequency is 928 MHz, and the wavelength of electromagnetic radiation in Space is 12 inches. The increase is due to variations in RSSI in the transition zone from near field to far field. Error bars show the standard deviations. The strength of the signal in mW as a function of the square of the distance is displayed in Figure 3-2. From the figure, the linear trend confirms the Friis free-space equation which predicts the attenuation of signal strength with increasing distance in the air.

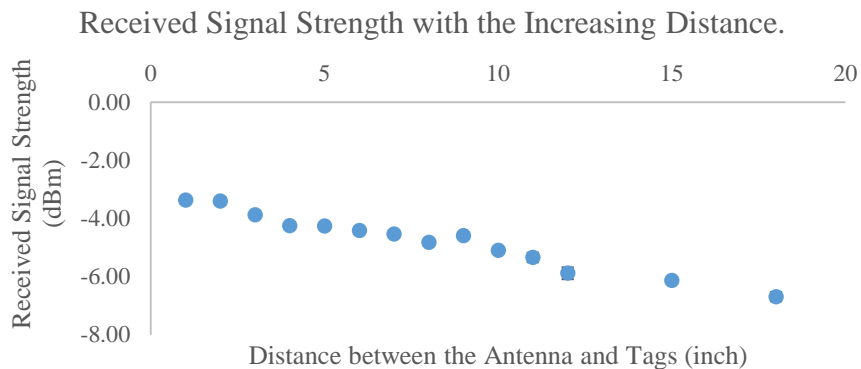


Figure 3-1. Decreasing received signal strength indicator with the distance.

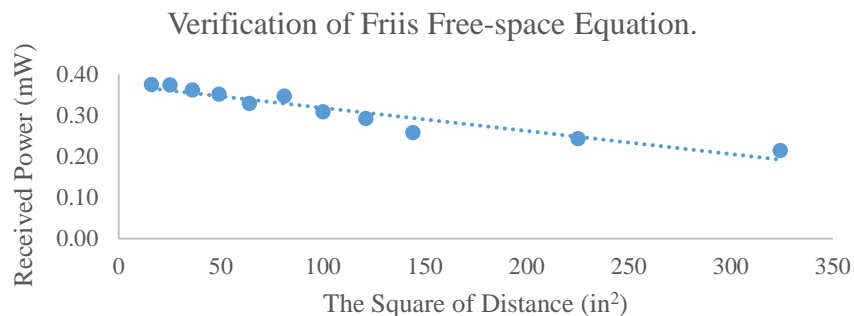


Figure 3-2. Verification of Friis free-space equation.

In the surface strain measurement of the aluminum beam, static equilibrium requires a constant shear and a linearly varying bending moment. The stress is uniaxial on the beam surface except the loading point and the clamped end. The measured strains from the RFID system from unloading to loading are shown below, and the average unloading strain measurement is calibrated to 0. The average loading strain is 196  $\mu\epsilon$ , very close to the calculated strain 191  $\mu\epsilon$ . Fluctuations of roughly 20 microstrains can be seen in Figure 3-3 when the beam is stable. Then, three steps loads were applied. The average RFID and wired strain measurements are shown in Figure 3-4. The measurements are identical, and both kinds of strain gauges show good linearity.

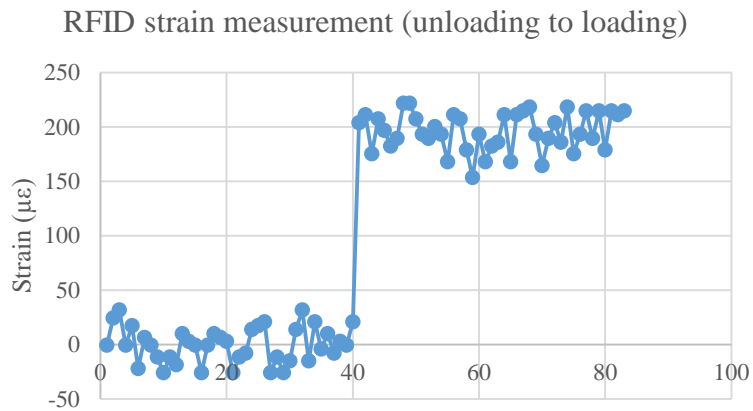


Figure 3-3. RFID strain measurement on the surface of the aluminum beam.

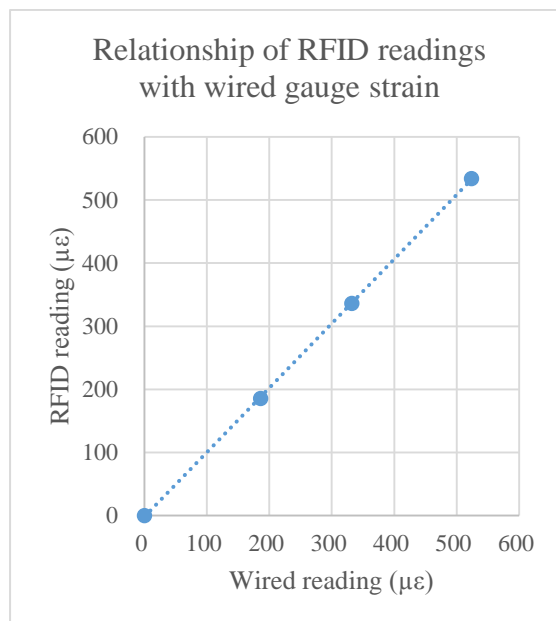


Figure 3-4. Comparison of strain measurement from RFID and wired gauges on the aluminum beam.

For the concrete beam, the compression test was performed using Forney loading machine<sup>38</sup>. The strain measurements have been averaged at various loads, and the stress-strain curves obtained from RFID and wired strain gauges are shown in Figure 3-5. The RFID strain measurements are 20 percent less than the wired strain measurements. In the compression test, end zones can develop caused by frictional end restraint, and a bulking-type failure may exhibit<sup>39</sup>. Therefore, the difference could result from the curvature developed along the surface of the concrete beam. Since the wired strain gauge is much longer than the RFID strain gauge, the curvature has greater effects on the wired strain gauge.

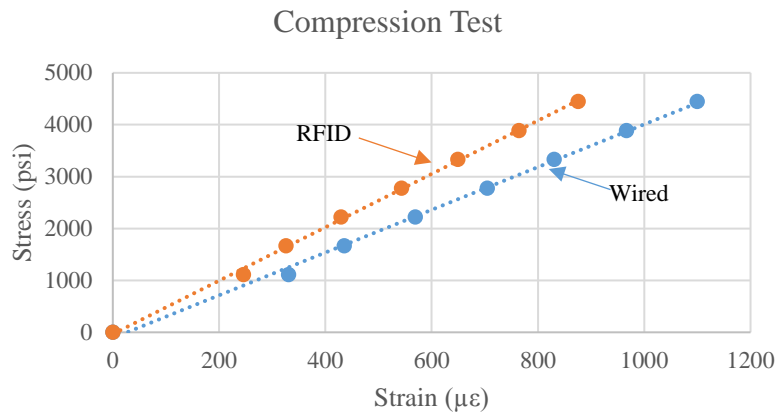


Figure 3-5. Stress-strain curves measured by RFID and wired strain.

When the RFID strain gauge was embedded in the mortar with the packaging technology, a wired strain gauge was attached on the surface for comparison. Compression test results show good linearity and a similar difference from the wired strain still exists. Drying shrinkage can be determined by the RFID and wired strain gauge, shown in Figure 3-6, and the received signal strength increases with the mortar age, shown in Figure 3-7. With the mortar aging, the degree of saturation decreases and the drying continues from the surface so that the received signal strength increases in the first few days to a stable level. The RFID sensor is in the center of the beam, and the relative humidity keeps 100% in the first two weeks. Therefore, the RFID strain measurements increase during this period.

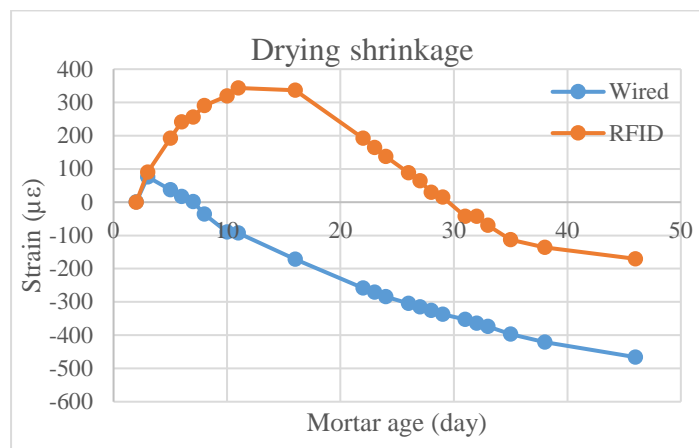


Figure 3-6. Drying shrinkage of a mortar beam.

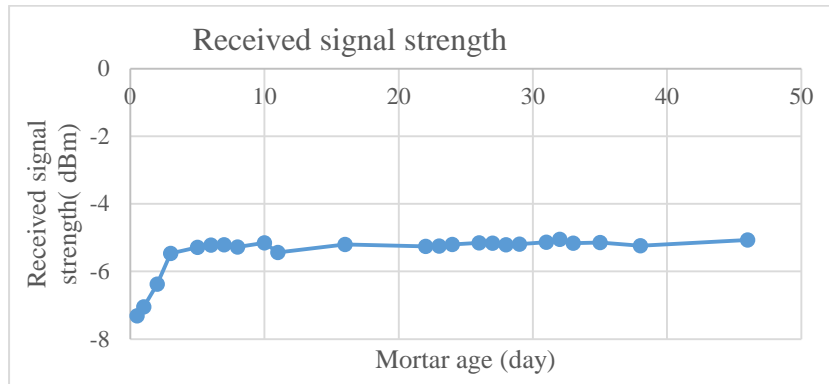
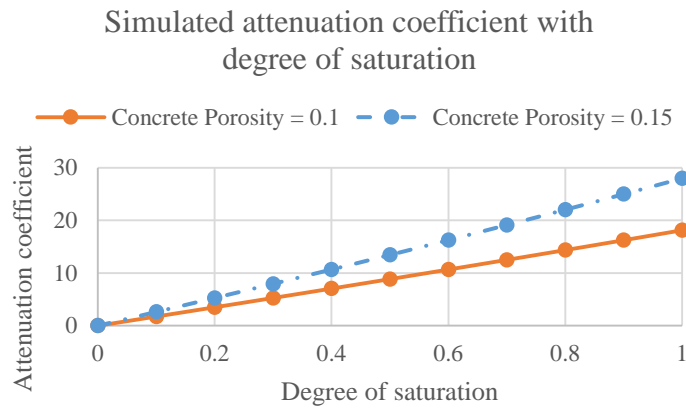


Figure 3-7. Received signal strength with the mortar age.

As a heterogeneous material, concrete can be simplified to a mixture of concrete solid, saline water, and air in terms of dielectric properties<sup>40</sup>. The effective electromagnetic properties of concrete can be derived from the known parameters of its constituents with proportions and spatial distributions<sup>40</sup>, for example, the Complex Refractive Index Model (CRIM)<sup>41</sup>. Figure 3-8 illustrates the outcome of models that show the ability to correlate signal strength with material properties. With the increasing degree of saturation, the conductivity of concrete will rise due to more ionic conduction in the solution. The concrete with 0.15 porosity will have more pore solution than the concrete with 0.1 porosity at the same degree of saturation, and therefore, the concrete will have larger loss factor and attenuation coefficient.



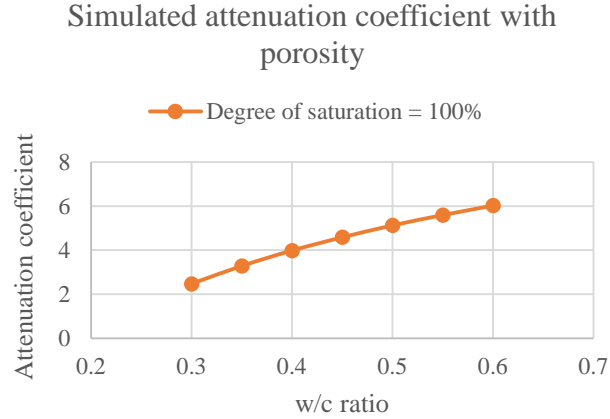


Figure 3-8. Modeling for attenuation coefficient with the degree of saturation for various concrete porosity and with varying w/c ratio.

In the experimental verification of the electromagnetic attenuation model, 1-inch and 2-inch thick high porosity paste samples are used. Also, 1-inch and 2-inch wide Acrylic tanks are used to determine the signal attenuation through pure water lime water. Figure 3-9 shows the signal strength through the 1 inch fully saturated paste samples and 1 inch water tank. For the paste samples with the porosity of 55% and 43%, there are some connected pores, so the water cannot fill all the porosity. For the paste sample with the porosity of 34%, the signal strength is close to that of lime water. With various degrees of saturation, the received signal strength can be seen in Figure 3-10 for these paste samples. Around 75% degree of saturation, all the samples have the largest signal attenuation. Also, the signal attenuation stays the same when the degree of saturation is below 25%. These findings may relate to the dielectric difference between the adsorbed water in concrete pores and the bulk water in the models. Figure 3-11 shows the received signal strength for 1 inch and 2 inch paste samples under oven-dried and fully saturated conditions.

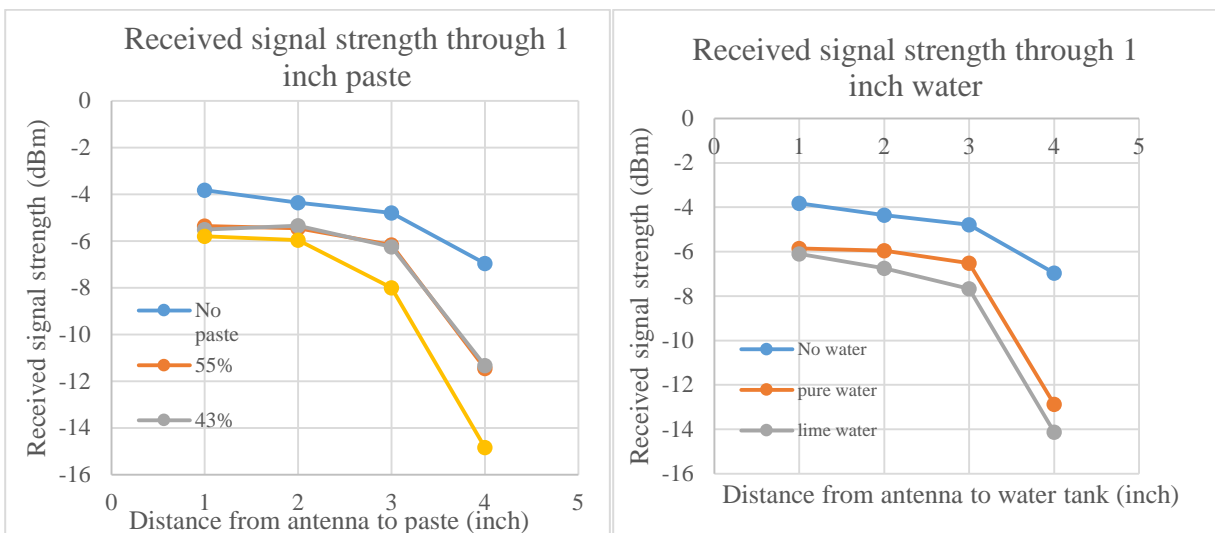


Figure 3-9. Received signal strength through 1 inch paste and water.

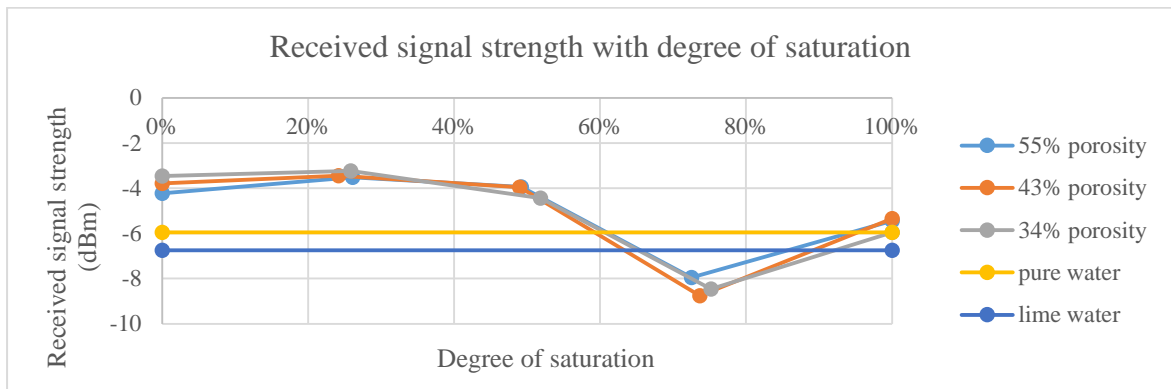


Figure 3-10. Received signal strength with various degrees of saturation.

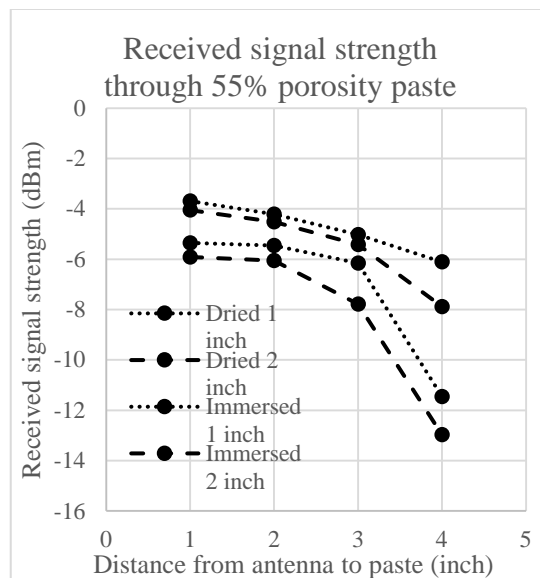


Figure 3-11. Received signal strength with different thickness.

### CHAPTER 3 – Findings

RFID technology can contribute to building a passive wireless sensor network. Various sensors monitoring structural health can be integrated with RFID tags, and RFID-based sensors can be incorporated into the commercial RFID systems. The low cost can make deploying massively distributed sensors practical. A passive wireless sensor system based on RFID technology has been utilized, and the performance regarding the measurement accuracy, speed, and range has been evaluated. RFID-based strain measurements have been compared with the conventional wired strain gauge on the aluminum and concrete beam. The results have shown good linearity and are consistent with the conventional wired strain measurements. RFID signal transmission between the reader and the tags has the effect on the system implementation. Therefore, the received signal strength transmitted from the tags is measured with the increasing transmission distance. Moreover, when RFID-based sensors are embedded in



concrete, the concrete as a dielectric medium can influence the transmitting waves. The electromagnetic property of concrete is investigated, and RFID signal attenuation in concrete is also simulated with various degree of saturation, porosity, and salt concentration. Experimental measurements have been performed to verify the simulation results. The drying shrinkage of early age mortar has been monitored by the passive wireless system.

More attenuation tests will refine the simulation model, and approximation equations will be suggested based on the attenuation experimental results to estimate the attenuation coefficient. The critical attenuation coefficient will be determined for the use of the RFID system. Therefore, complex simulations will be avoided for engineering reality, and appropriate w/cm ratios, concrete porosity, and embedment depth will be recommended. Future work will include field testing in pavements at O'Hare Int'l Airport. RFID electronics will be embedded in recycled aggregate concrete on field sites, and the measurements will be recorded during a winter in Chicago. The reliability of long-term operation could be evaluated in the freeze-thaw cycles.

## Reference

1. Van Der Auweraer, H. & Peeters, B. Sensors and systems for structural health monitoring. *Journal of Structural Control* **10**, 117–125 (2003).
2. Ko, J. M. & Ni, Y. Q. Technology developments in structural health monitoring of large-scale bridges. *Eng. Struct.* **27**, 1715–1725 (2005).
3. Mukhopadhyay, S. C. & Ihara, I. Sensors and technologies for structural health monitoring: A review. *Lecture Notes in Electrical Engineering* **96**, 1–14 (2011).
4. Celebi, M. Seismic instrumentation of buildings (with emphasis on federal buildings). *Technical Report No. 0-7460-68170* (2002).
5. Lynch, J. P. & Loh, K. J. A Summary Review of Wireless Sensors and Sensor Networks for Structural Health Monitoring. **38**, (2006).
6. Lynch, J. P. An overview of wireless structural health monitoring for civil structures. *Philos. Trans. R. Soc. A Math. Phys. Eng. Sci.* **365**, 345–372 (2007).
7. Anton, S. R. & Sodano, H. A. A review of power harvesting using piezoelectric materials (2003–2006). *Smart Mater. Struct.* **16**, R1–R21 (2007).
8. Deivasigamani, A., Daliri, A., Wang, C. H. & John, S. A review of passive wireless sensors for structural health monitoring. *Modern Applied Science* **7**, 57–76 (2013).
9. Zhang, J., Tian, G., Marindra, A., Sunny, A. & Zhao, A. A review of passive RFID tag antenna-based sensors and systems for structural health monitoring applications. *Sensors* **17**, 265 (2017).
10. Krüger, M., Grosse, C. U. & Marrón, P. J. Wireless structural health monitoring using MEMS. *Key Eng. Mater.* **293–294**, 625–634 (2005).
11. Ceylan, H. *et al.* Highway infrastructure health monitoring using micro-electromechanical sensors and systems (MEMS). *J. Civ. Eng. Manag.* **19**, S188–S201 (2013).
12. Virtanen, J., Ukkonen, L., Björninen, T., Elsherbeni, A. Z. & Sydänheimo, L. Inkjet-printed humidity sensor for passive UHF RFID systems. in *IEEE Transactions on Instrumentation and Measurement* **60**, 2768–2777 (2011).
13. Manzari, S. *et al.* Humidity sensing by polymer-loaded UHF RFID antennas. *IEEE Sens. J.* **12**, 2851–2858 (2012).

14. Gao, J., Siden, J., Nilsson, H. E. & Gulliksson, M. Printed humidity sensor with memory functionality for passive RFID tags. *IEEE Sens. J.* **13**, 1824–1834 (2013).
15. Amin, E. M., Bhuiyan, M. S., Karmakar, N. C. & Winther-Jensen, B. Development of a low cost printable chipless RFID humidity sensor. *IEEE Sens. J.* **14**, 140–149 (2014).
16. You, Z., Mills-Beale, J., Pereles, B. D. & Ong, K. G. A wireless, passive embedded sensor for real-time monitoring of water content in civil engineering materials. *IEEE Sens. J.* **8**, 2053–2058 (2008).
17. Girbau, D., Ramos, Á., Lazaro, A., Rima, S. & Villarino, R. Passive wireless temperature sensor based on time-coded UWB chipless RFID tags. *IEEE Trans. Microw. Theory Tech.* **60**, 3623–3632 (2012).
18. Amendola, S., Bovesecchi, G., Palombi, A., Coppa, P. & Marrocco, G. Design, calibration and experimentation of an epidermal RFID sensor for remote temperature monitoring. *IEEE Sens. J.* **16**, 7250–7257 (2016).
19. Noor, T., Tenhunen, H., Habib, A., Amin, Y. & Loo, J. High-density chipless RFID tag for temperature sensing. *Electron. Lett.* **52**, 620–622 (2016).
20. Pour-Ghaz, M. *et al.* Wireless crack detection in concrete elements using conductive surface sensors and radio frequency identification technology. *J. Mater. Civ. Eng.* **26**, 923–929 (2014).
21. Merilampi, S., Björninen, T., Ukkonen, L., Ruuskanen, P. & Sydänheimo, L. Embedded wireless strain sensors based on printed RFID tag. *Sens. Rev.* **31**, 32–40 (2011).
22. Mohammad, I. & Huang, H. An antenna sensor for crack detection and monitoring. *Adv. Struct. Eng.* **14**, 47–53 (2011).
23. Xu, X. & Huang, H. Multiplexing passive wireless antenna sensors for multi-site crack detection and monitoring. *Smart Mater. Struct.* **21**, 15004 (2012).
24. Kalansuriya, P., Bhattacharyya, R. & Sarma, S. RFID tag antenna-based sensing for pervasive surface crack detection. *IEEE Sens. J.* **13**, 1564–1570 (2013).
25. Caizzone, S., DiGiampaolo, E. & Marrocco, G. Wireless crack monitoring by stationary phase measurements from coupled RFID tags. *IEEE Trans. Antennas Propag.* **62**, 6412–6419 (2014).
26. Cazeca, M. J., Mead, J., Chen, J. & Nagarajan, R. Passive wireless displacement sensor based on RFID technology. *Sensors Actuators A Phys.* **190**, 197–202 (2013).
27. Paggi, C., Occhiuzzi, C. & Marrocco, G. Sub-millimeter displacement sensing by passive UHF RFID antennas. *IEEE Trans. Antennas Propag.* **62**, 905–912 (2014).
28. Lesthaeghe, T., Frishman, S. & Holland, S. D. *RFID Tags for Detecting Concrete Degradation in Bridge Decks. InTrans Project Reports* (2013).
29. Watters, D. G., Bahr, A. J., Jayaweera, P. & Huestis, D. L. *SMART PEBBLES™: Passive Embeddable Wireless Sensors for Chloride Ingress Monitoring in Bridge Decks.* (2003).
30. Cain, R., Carkhuff, B., Pandolfini, P. & Weiskopf, F. *Smart Aggregate Sensor Suite for Bridge Deck Measurement-Phase I.* (2003).
31. Bhadra, S., Thomson, D. J. & Bridges, G. E. A wireless embedded passive sensor for monitoring the corrosion potential of reinforcing steel. *Smart Mater. Struct.* **22**, 75019 (2013).
32. Khalifeh, R. *et al.* Development of wireless and passive corrosion sensors for material degradation monitoring in coastal zones and immersed environment. *IEEE J. Ocean. Eng.* **41**, 776–782 (2016).
33. Sunny, A. I., Tian, G. Y., Zhang, J. & Pal, M. Low frequency (LF) RFID sensors and selective transient feature extraction for corrosion characterisation. *Sensors Actuators, A Phys.* **241**, 34–43 (2016).

34. Zhang, H. *et al.* Identification and characterisation of steel corrosion using passive high frequency RFID sensors. *Measurement* **92**, 421–427 (2016).
35. Manzari, S. *et al.* A passive temperature radio-sensor for concrete maturation monitoring. in *2014 IEEE RFID Technology and Applications Conference, RFID-TA 2014* 121–126 (IEEE, 2014). doi:10.1109/RFID-TA.2014.6934212
36. Nummela, J., Ukkonen, L. & Sydänheimo, L. The effect of low temperature on passive UHF RFID tags. in *Proceedings of the 4th WSEAS International Conference on REMOTE SENSING (REMOTE'08)* (ed. S.C. Misra) 88–92 (2008).
37. Sbartäi, Z. M., Laurens, S., Balayssac, J. P., Ballivy, G. & Arliguie, G. Effect of concrete moisture on radar signal amplitude. *ACI Mater. J.* **103**, 419–426 (2006).
38. Compression Machines | FORNEY LP | FORNEY LP. Available at: <https://www.forneyonline.com/machine-types/compression-machines>. (Accessed: 1st December 2017)
39. Bischoff, P. & Perry, S. Impact behavior of plain concrete loaded in uniaxial compression. *J. Eng. Mech.* **121**, 685–693 (1995).
40. Tsui, F. & Matthews, S. L. Analytical Modelling of the Dielectric Properties of Concrete for Subsurface Radar Applications. *Consrrucjion Build. Moter.* **11**, 149–161 (1997).
41. Udaya B. Halabe, Arash Sotoodehnia, Kenneth R. Maser, and E. A. K. Modeling of the Electromagnetic Properties of Concrete. *ACI Mater. J.* **90**, 552–563 (1993).